Electronic Supplementary Material (ESI) for Physical Chemistry Chemical Physics.

Supplementary Information to

Ligand-modulated interactions between charged monolayer-protected $Au_{144}(SR)_{60}$ gold nanoparticles in physiological saline

Oscar D Villarreal, Liao Y Chen, Robert L Whetten and Miguel J Yacaman

In Fig. S1, we illustrate the structures of the $Au_{144}S_{60}$ core and the 5 charged thiolate groups employed.

In Fig. S2, we illustrate the building of the $pMBM^{+}$-AuNP.

In Fig. S3, we illustrate the multi-sectional scheme employed to calculate the PMF of the AuNP pairs as a function of the distance between their centers of mass.

In Fig. S4, we compare the density distributions of terminal groups and ions for each NP system.

In Fig. S5, we compare the density distributions of the ions whose charge sign is common to that of the terminal groups.

In Fig. S6, we fit the counter-ion density distributions to the Debye-Hückel description.

In Fig. S7, we plot the mean squared displacement (MSD) of an ion (Na^{+} or Cl^{-}) for the entire simulation time interval (20 ns) for each system. The statistical averages are over the whole trajectories of all the Na^{+}/Cl^{-} ions for each system. The second plot is the ion MSDs over a time interval of 0.1 ns with statistics over 200 short trajectories (0.1 ns segments of the 20 ns trajectory) for each ion and over all the Na^{+}/Cl^{-} ions for each system. The third plot presents the expression MSD(t)/6t.

In Fig. S8, we present the configuration of minimum energy for the binding of the terminal groups to the counterions, when considering only the electrostatic and van der Waals forces, and without considering water.

Table S1 presents the CHARMM parameters of the terminal groups and counterions.

In Fig. S9, we plot the work done to the systems along the pulling paths of SMD runs.

In Fig. S10, we show snapshots at the long range separation between the AuNPs.

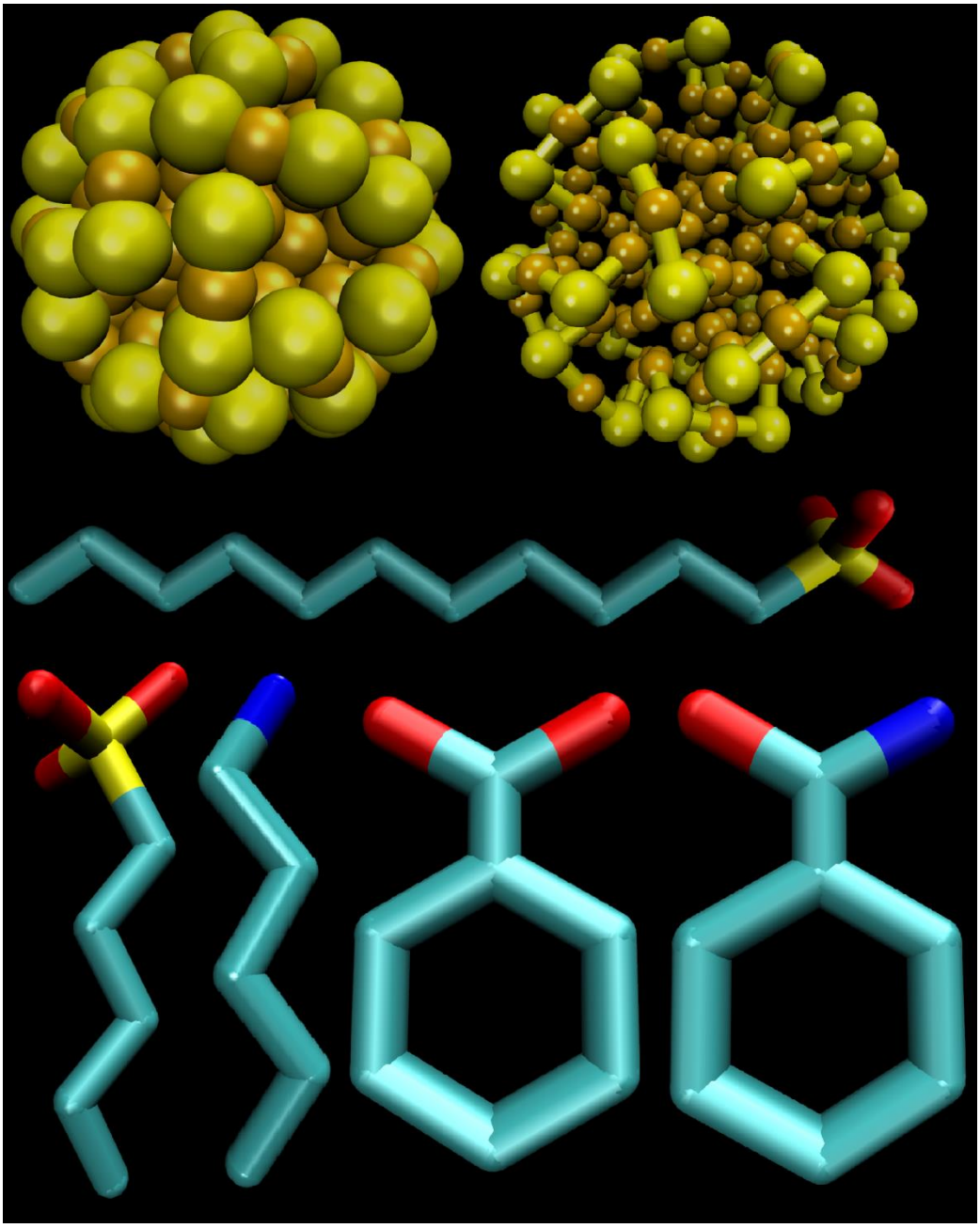

Fig. S1. The Au-S core shown in balls (top left) and in balls and ball-and-sticks (top right). The ligand R-group structures (hydrogen and thiolate-sulfur are omitted): 11-mercapto-1-undecanesulfonate ("MUS", $C_{11}H_{22}SO_3$, charge = −1e) (center); 5-mercapto-1-pentanesulfonate ("MPS", $C_5H_{10}SO_3$, charge = -1 e), bottom left; 5-mercapto-1-pentaneamine ("MPM", $C_5H_{10}NH_3$, charge = +1e), bottom second from left; 4-mercapto-benzoate ("pMBA" $C_7H_4O_2$, charge = −1e), bottom second from right; 4-mercapto-benzamide ("pMBM" $C_7H_4ONH_3$, charge = +1e), bottom right. S: Yellow. Au: Gold. C: Cyan. O: Red. N: Blue.

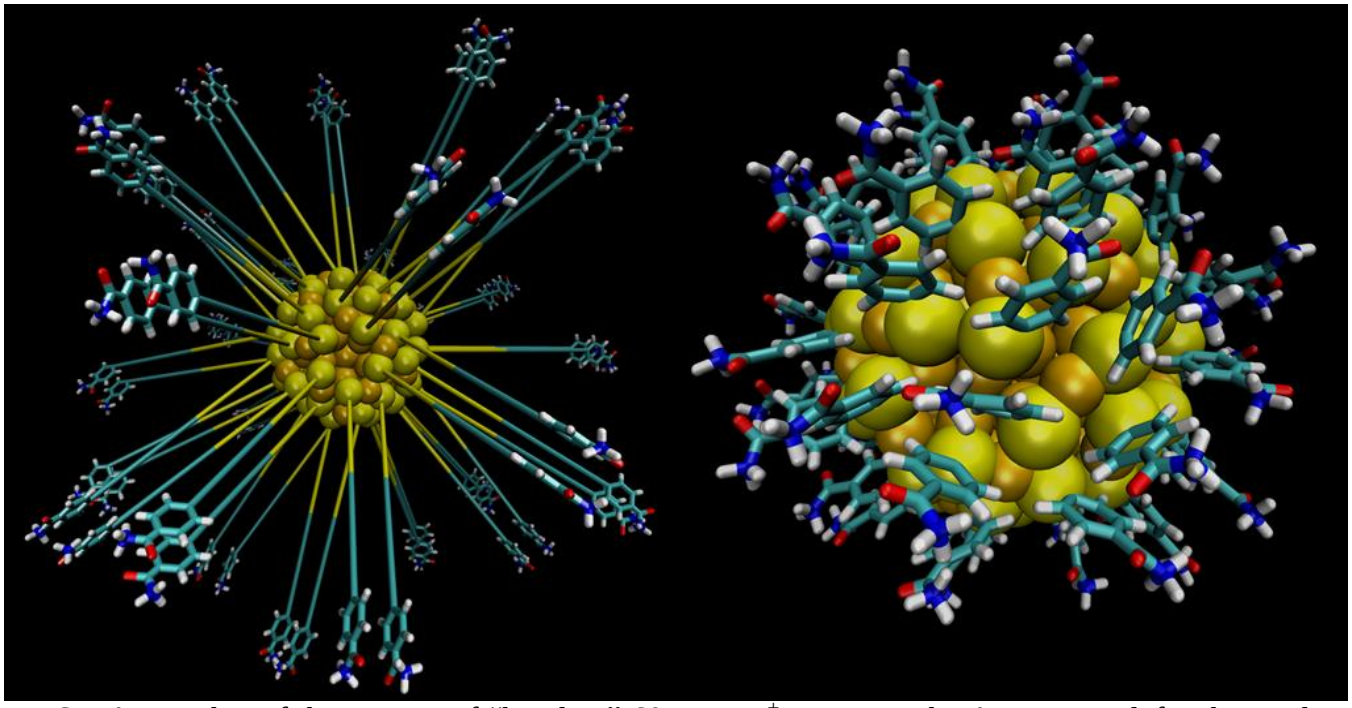

Fig S2. A snapshot of the process of "bonding" 60 $pMBM^+$ groups to the AuNP core, left. The product of the "bonding" process---a functionalized AuNP (structure optimized in vacuum), right.

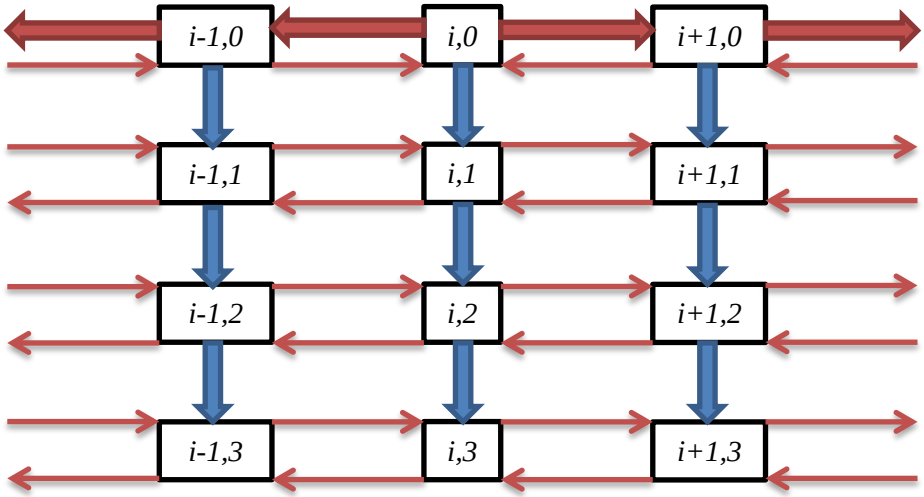

Fig. S3. The multi-sectional scheme employed. The starting point is the state labeled *"i,0"* (section *i*, path 0), and was obtained after equilibrating the system for 20 ns with the centers of mass (COM) of the inner most AU cores (12 Au atoms in each NP) fixed at z = ± 2.5 nm, respectively. The blue arrows represent 10 ps of equilibration, employed to generate the *"i,j+1"* state. The broad red arrows represent 0.1 ns of dragging the COM of each particle forwards/backwards at a speed of 1 nm/ns (for a total of 0.1 nm), followed by 1 ns of equilibration to generate the *"i±1,j"* state. The narrow red arrows represent the same drag as the broad arrows, but without equilibrating the state at the end.

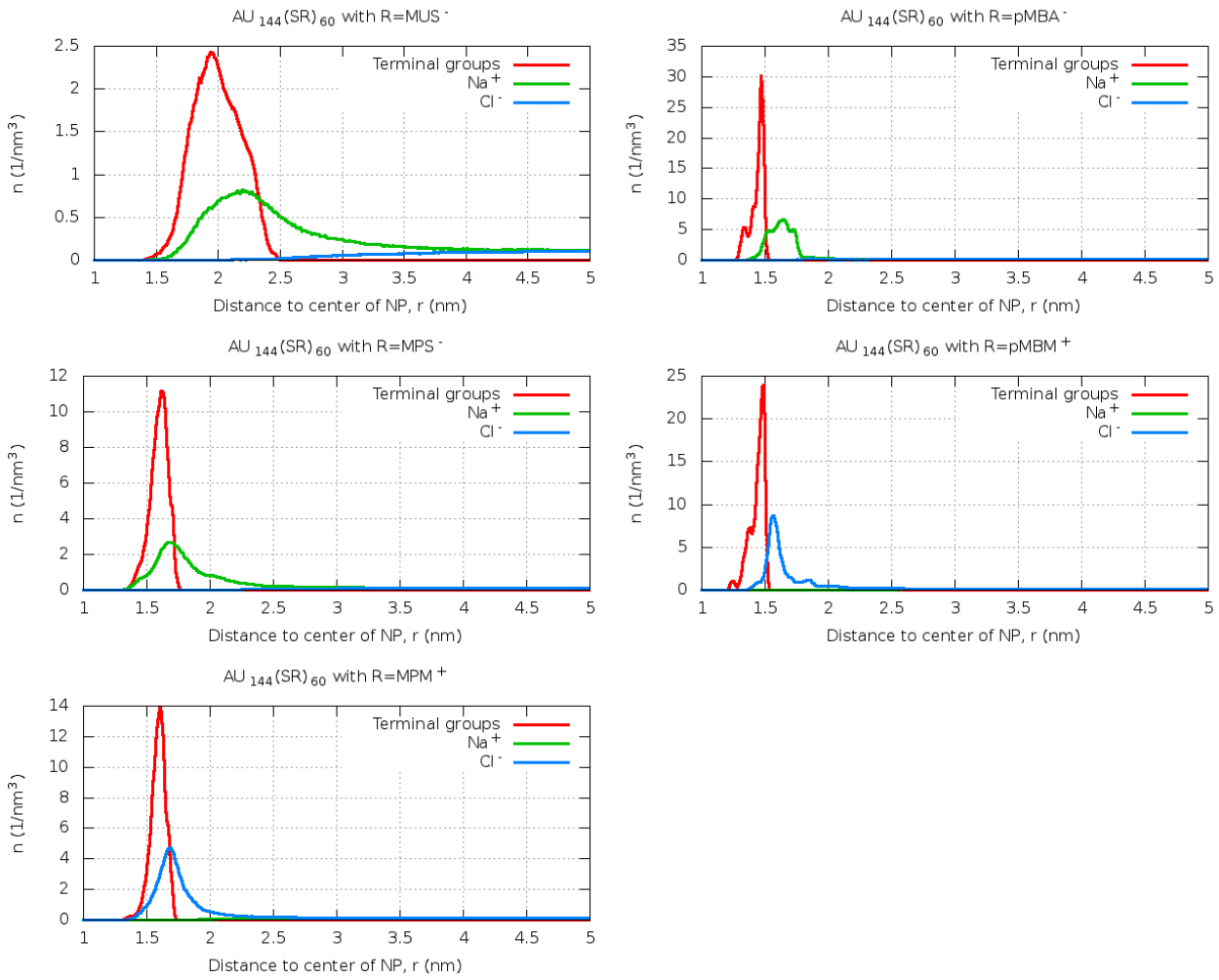

Fig. S4. Comparison between the density distributions of terminal groups and ions for each NP.

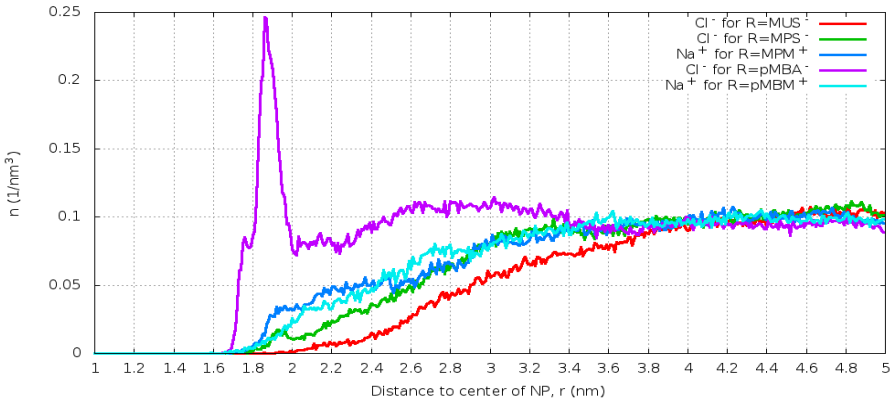

Fig. S5. The density distributions of the ions whose charge sign is common to that of the terminal groups. Note the peak of Cl^- in the $pMBA^-$ case at ≈ 1.9 nm, which indicates that the Na^+ counter-ion shell (whose peak laid at ≈ 1.6 nm) was rigid enough to allow the formation of an adjacent shell of Cl^- ions whose peak was, however, much smaller than that of Na^+.

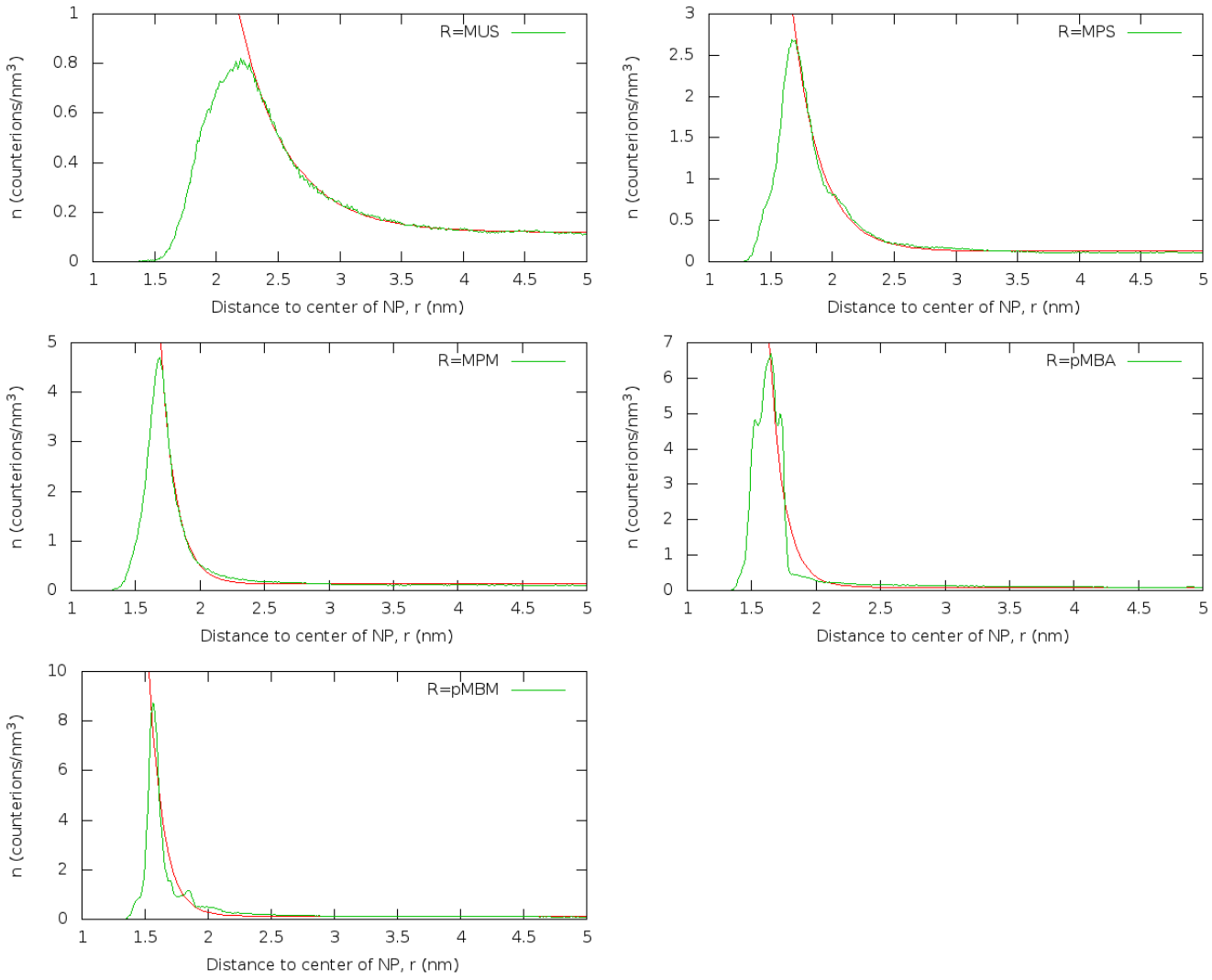

Fig. S6. The counterion density distributions fitted to the Debye-Hückel description around a charged nanoparticle. The resulting Debye lengths were: 0.47 nm, MUS; 0.26 nm, MPS; 0.13 nm, MPM; 0.12 nm, pMBA; 0.12 nm, pMBM. The RMS of the residuals of the fitting were: 0.0068, MUS; 0.036, MPS; 0.035, MPM; 0.27, pMBA; 0.24, pMBM. Therefore, the less the ligand fluctuated (i.e. the shorter and less flexible it was), the more the counterion distribution distanced itself from the Debye-Hückel description.

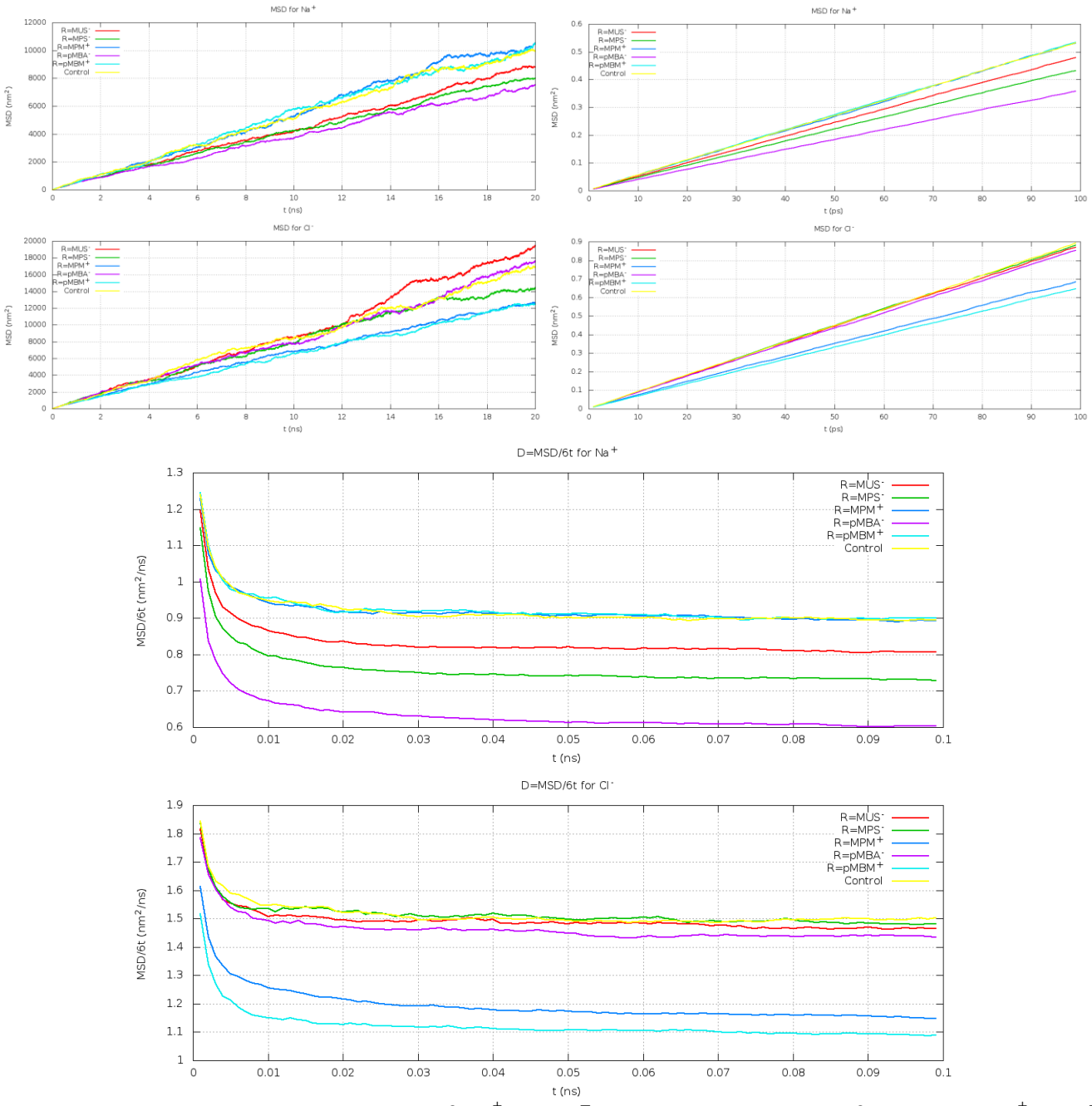

Fig. S7. The mean squared displacement of Na^+ and Cl^- averaged over all ions of each type (Na^+ or Cl^-) for the entire trajectory of 20 ns simulation, top left. The Mean Squared Displacement of the Na^+ and Cl^- ions, calculated from short time-intervals (100 ps), and averaging over 200 short trajectories of 100 ps each, top right. The convergence of the diffusion coefficient: D=MSD(t)/6t calculated for the folded trajectories, bottom. There are no nanoparticles present in the control group. Note how the ions with the smallest diffusion coefficient are the Na^+ in the pMBA case. In that case, some of the 60 Na^+ counter-ions are essentially non-diffusive and non-exchanging with the Na^+ in the medium. One could thus call them "structural" or "contact-ion pairs".

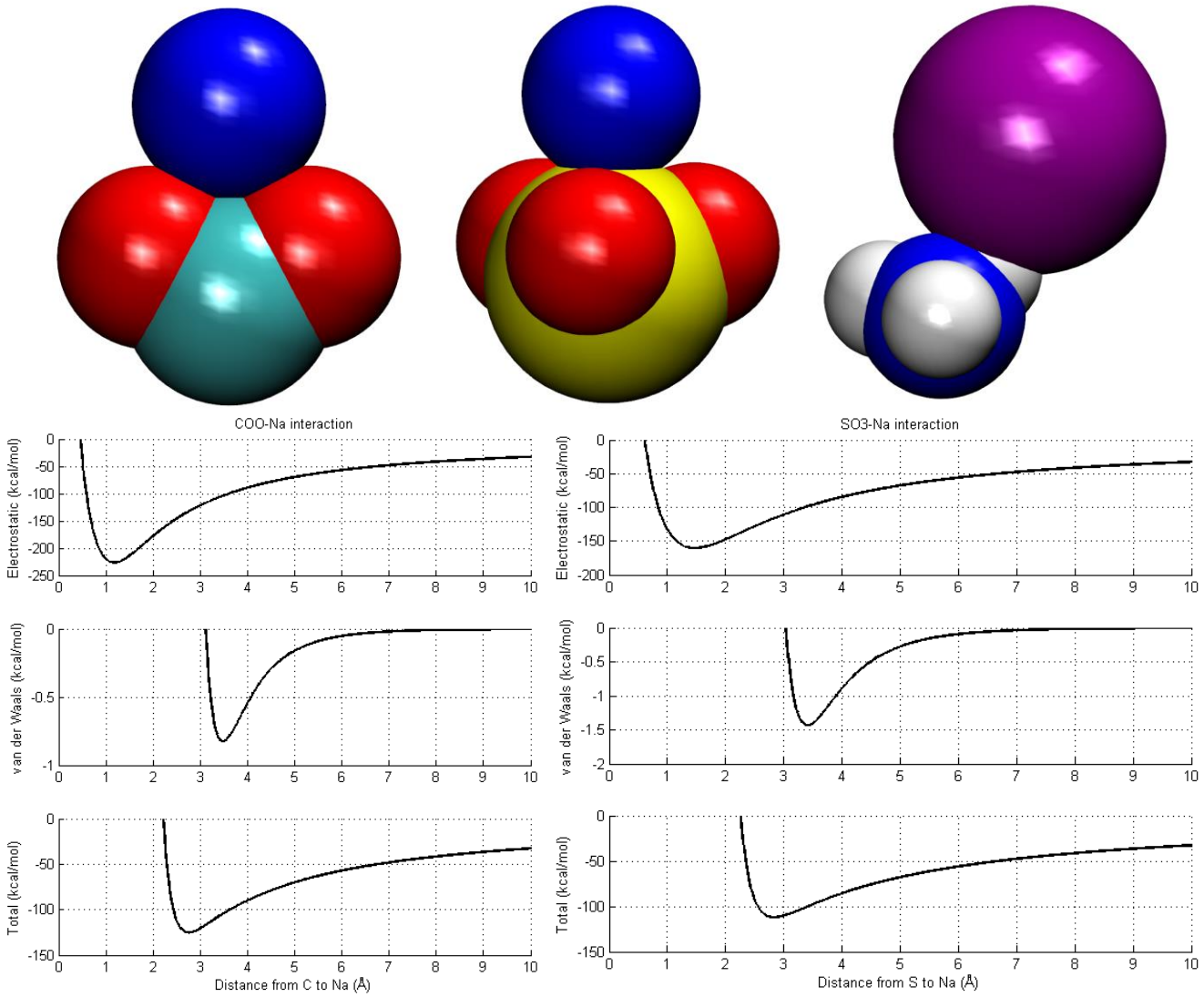

Fig. S8. The water-free configuration of minimum energy for the binding of the terminal groups to the counterions, when considering only the electrostatic and van der Waals forces: Na^+-COO^-, with a COM separation between C and Na of 2.75 Å, top left; Na^+-SO_3^- with a S-Na separation of 2.83 Å, top middle; Cl^--NH_3^+, with a N-Cl separation of 3.31 Å, top right. The electrostatic and van der Waals energies of Na^+ when interacting with COO^-, as a function of the distance between C and Na^+, bottom left; or with SO_3^-, as a function of the distance between S and Na^+, bottom right.

Table S1. CHARMM parameters employed for the terminal groups and counterions.

	COO^-		SO_3^+		NH_3^+		Counterions	
	C	**O**	**S**	**O**	**N**	**H**	Na^+	Cl^-
Q(e)	0.62	-0.76	0.73	-0.55	-0.3	0.33	1	-1
ϵ (kcal/mol)	-0.07	-0.12	-0.47	-0.12	-0.2	-0.046	-0.0469	-0.15
$r_{min}/2$ (Å)	2	1.7	2.1	1.7	1.85	0.2245	1.41075	2.27
Bond length (Å)	1.26 (CO)		1.448 (SO)		1.04 (NH)			
Angle (°)	124 (OCO)		109.47 (OSO)		109.5 (HNH)			

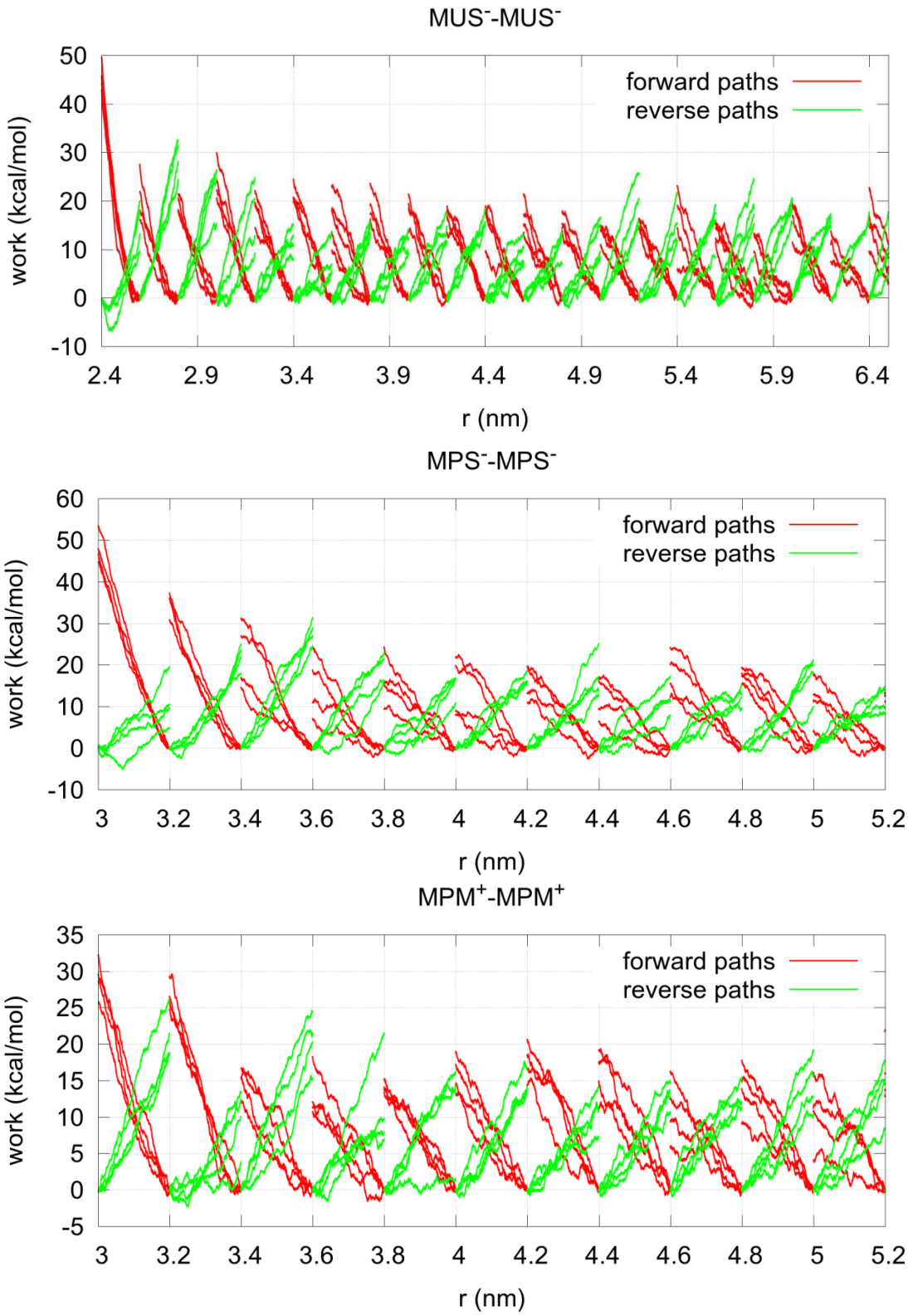
MUS⁻-MUS⁻
work (kcal/mol)
r (nm)
forward paths
reverse paths
MPS⁻-MPS⁻
work (kcal/mol)
r (nm)
forward paths
reverse paths
MPM⁺-MPM⁺
work (kcal/mol)
r (nm)
forward paths
reverse paths

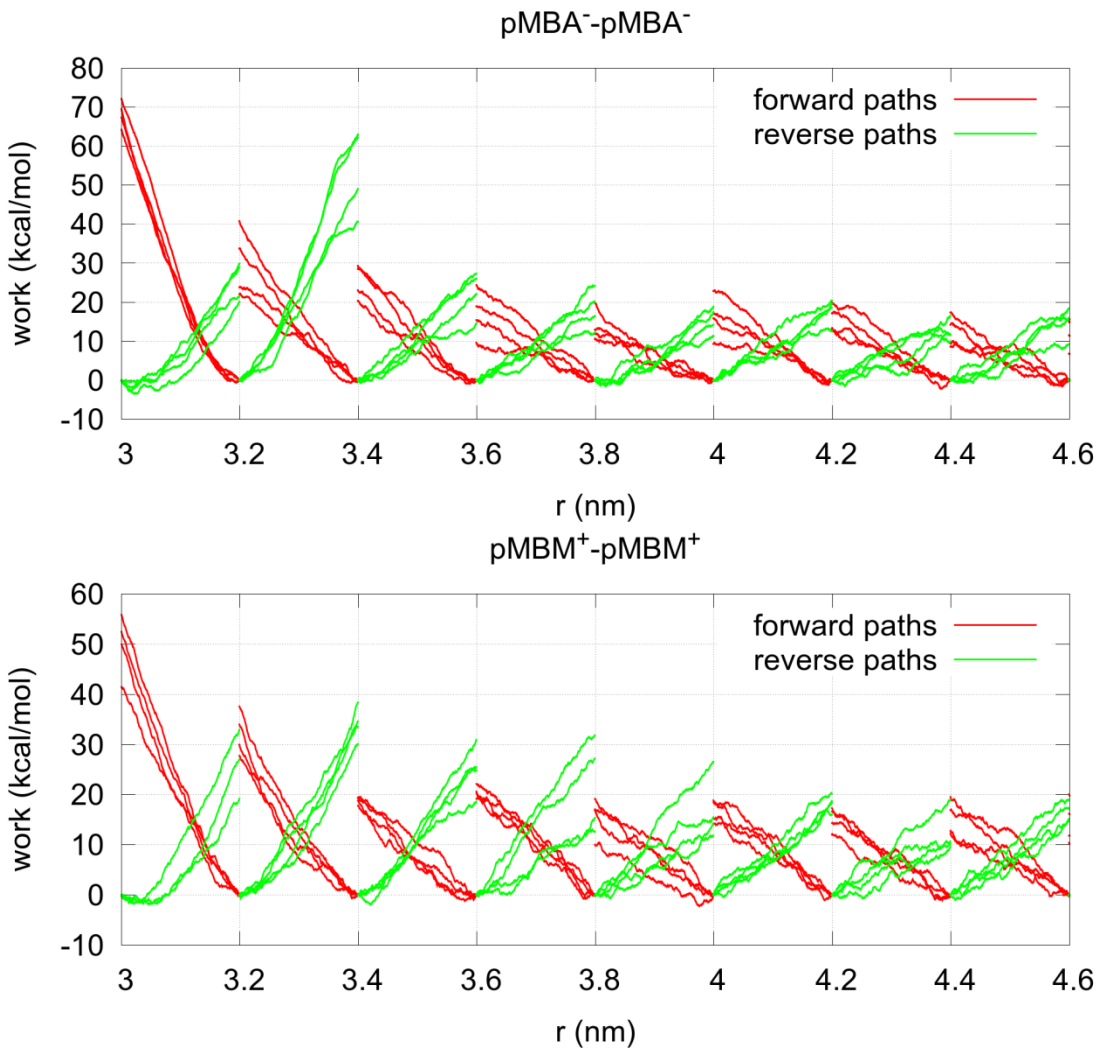

Fig. S9. The work along forward (red) and reverse (green) paths of pulling two AuNPs together as a function of the distance (r) between the centers of mass of the Au cores of the two AuNPs.

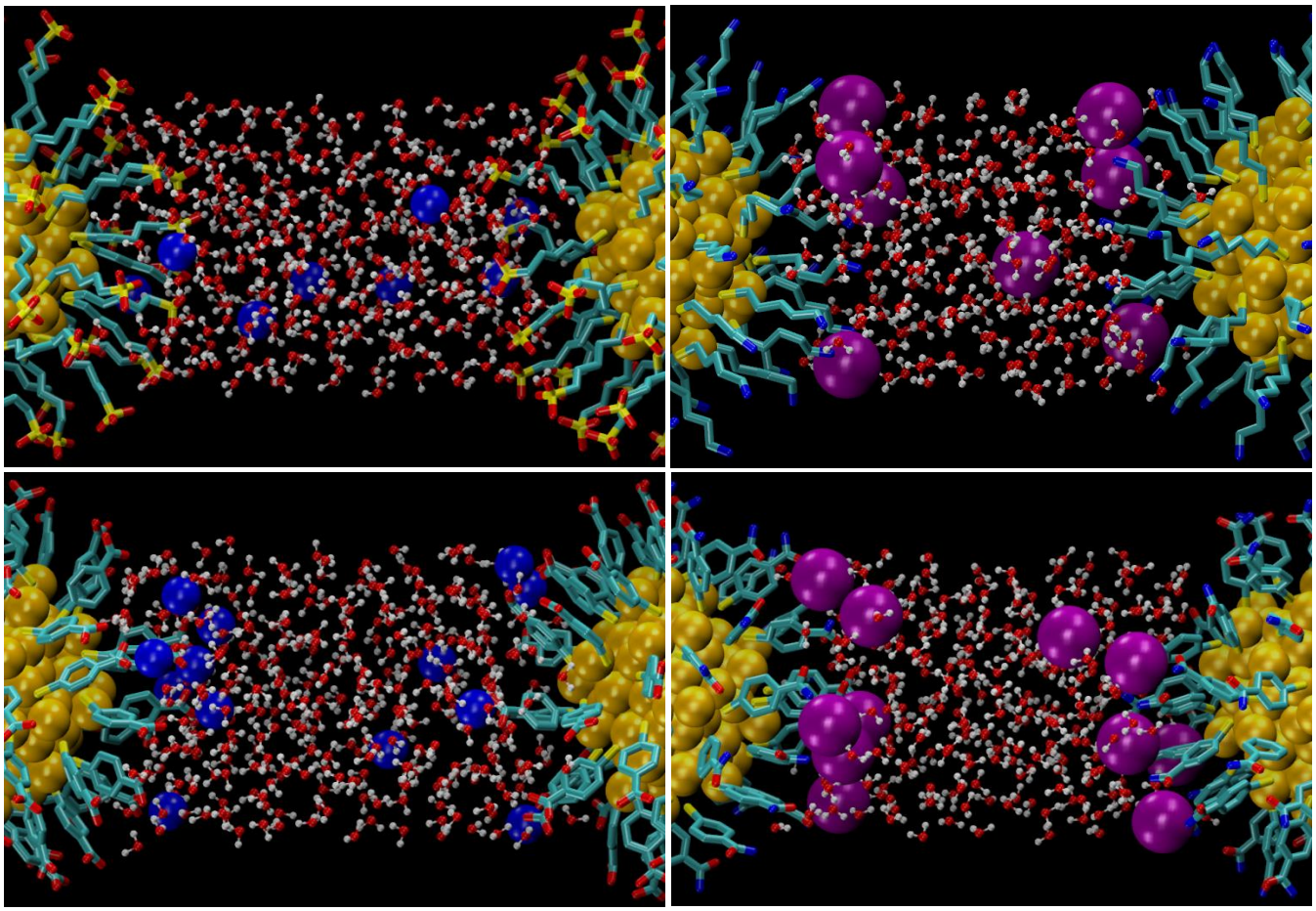

Fig. S10. Snapshots at the long range separation between the: MPS^--MPS^-, top left; MPM^+- MPM^+, top right; $pMBA^-$- $pMBA^-$, bottom left; and $pMBM^+$- $pMBM^+$, bottom right.